Joint Centre for Mesoscale Meteorology, Reading, UK

The Objective Analysis of Dropsonde Data from FASTEX

N. Roberts
R. Forbes
S. Clough
M. Dixon
A. Macallan

Internal Report No. 106

January 2000

Met Office Joint Centre for Mesoscale Meteorology Department of Meteorology
University of Reading PO Box 243 Reading RG6 6BB United Kingdom
Tel: +44 (0)118 931 8425 Fax: +44 (0)118 931 8791
www.metoffice.com

Designed and produced by the Met Office © Crown copyright 2001 01/0240 The Met Office logo is a registered trademark.

The Objective Analysis of Dropsonde Data from FASTEX

Richard Forbes[1], Sid Clough[1], Mark Dixon[2],
Andy Macallan[1], Nigel Roberts[1]

[1] JCMM, Meteorological Office
[2] JCMM, University of Reading

Abstract

This report documents the objective analysis method used to form gridded cross-sections from dropsonde data collected during the Fronts and Atlantic Storm Track Experiment (FASTEX). The processing of the dropsonde data, the characteristics of the analysis method and sensitivities to parameter variations are described. The use of an isentropic vertical coordinate rather than a pressure coordinate is found to improve the analyses. Overall, the objective analysis of dropsonde data is able to provide spatially coherent fields with useful information on mesoscale structures.

1. Introduction

During the Fronts and Atlantic Storm Track Experiment (FASTEX, Joly et al. 1997) the UK C-130 and US P-3 aircraft provided dropsonde data for many of the Intensive Observing Periods (IOPs). Sondes were dropped from a height of around 8km at approximately 50km intervals along a series of flight legs, each a few hundred kilometres long. For the analysis of the data it is useful to visualise the coherence of features in the dropsonde observations by spatial interpolation in a vertical plane along each leg of the flight path. This interpolation can be performed objectively using one of a variety of data analysis methods (e.g. Daley 1991). One relatively simple and computationally efficient technique is that of successive corrections (Cressman 1959, Bratseth 1986). Pedder (1993) applies such a technique based on the method of Bratseth (1986) to an analysis of scattered observations for which there is no background field, and this technique is used here for the analysis of FASTEX dropsonde data. Pressure is directly measured by the dropsondes and so is perhaps a natural vertical coordinate for the analysis, but atmospheric flow and anomaly correlations do not necessarily follow pressure surfaces. Alternative analysis coordinates such as isentropic or momentum surfaces can improve atmospheric analyses, particularly in frontal regions (Desroziers and Lafore 1993, Shapiro and Hastings 1973) and both pressure and isentropic coordinates are compared in this report. Section 2 describes the dropsonde data and preliminary processing as well as the *in situ* data from the aircraft which is included in the analyses. Section 3 outlines the objective analysis technique and Section 4 discusses the characteristics of the analysis method, impact of vertical coordinate and sensitivities to parameter variations. Section 5 provides a concluding summary.

2. Data and Preliminary Processing

2.1 Dropsonde Data

The dropsondes from the UK C-130 aircraft during FASTEX were RD82 GPS dropsondes developed by Vaisälä and flight-tested by the U.K. Meteorological Office with GPS (Global Positioning System) or LORAN winds. The temperature and humidity elements on these sondes were capacitative sensors as in the standard RS80 radiosonde, while the pressure sensor was a Barocap silicon pressure transducer as in the RS90 radiosonde. GPS winds were provided by a Vaisälä GPS111 receiver module on board the sondes with Vaisälä NWG201 processor cards on board the aircraft. The dropsondes typically take about 12 minutes to fall from an aircraft level of around 360hPa.

Processing of the dropsonde data is performed separately for the wind data (GPS) and for the pressure, temperature, and humidity data (PTU). The dropsondes transmit PTU data via six frequencies. A median filter is applied to the raw data and any points with gross error are flagged. A manual quality control check is then performed to flag any bad observations missed by the objective quality control. The pressure data are smoothed using a cubic spline approximation and coefficients supplied by Vaisälä are applied to the frequencies to generate the actual pressure, temperature and relative

humidity values. A final manual quality control check flags any remaining spurious points.

The wind data are derived from GPS measurements and a manual quality control check is used to reject spurious data. The remaining data profile is then smoothed by applying a regression fit over a running twenty second mean. The primary reason for smoothing the data is to remove horizontal oscillations of the dropsonde that can occur during the descent.

The resulting quality controlled PTU and GPS dataset contains vertical profiles of pressure, temperature, relative humidity, wind speed and wind direction with values nominally every 1.5 seconds. A further processing step removes relative humidity data in the first 40hPa of the dropsonde descent to take into account the time for the sensor to adjust from the relatively dry conditions of the aircraft to the environmental conditions. In contrast the temperature and wind measurements adjust to the environment quickly and this information is retained in the profiles.

2.2 Aircraft Data

The UK-C130 aircraft has instruments to measure *in situ* temperature (Harmer et al. 1990), wind (Offiler et al. 1994) and dew point (Rogers 1995) and these data are used to extend the dropsonde profiles up to the level of the aircraft. At the time of each dropsonde release, a 60 second average of the aircraft temperature, wind and derived relative humidity measurements are calculated (this corresponds to an average horizontal distance of about 6km). These values are then included at the top of the dropsonde profiles.

2.3 Filtering the Data

A final processing step is performed on each dropsonde profile to average the data in the vertical onto a series of specified pressure or isentropic levels (i.e. dry-bulb (θ) or wet-bulb (θ_w) potential temperature levels). It is these filtered data that are subsequently used in the objective analyses. The present implementation of the filter consists of simple layer averaging for each specified level. One potential problem with the θ and θ_w vertical coordinate is that vertical gradients can be very small, zero or even negative (for θ_w) in parts of the profile and it can become difficult to define a regularly spaced monotonically increasing vertical coordinate with such data. The filtering/interpolation process circumvents this problem by working downwards from the top of a dropsonde profile to determine the first occurrence of the specified levels. This forces the vertical coordinate to be single-valued but may leave certain regions of the domain with widely spaced levels if the vertical gradients are weak. This turns out to only be a problem for the moist isentropic coordinate where the vertical θ_w gradient is negative in a significant proportion of profiles (see Section 4 for a further discussion).

3. Objective Analysis

The objective analysis method is based on the iterative successive correction technique described in Pedder (1993; hereafter referred to as P93) and approximates an optimal interpolation of scattered observations within a limited domain. An outline of the scheme is given in this section but P93 should be referred to for a mathematical derivation and detailed description of the scheme.

3.1 Analysis Domain Definition

The analysis domain is defined as a vertical plane orientated along a specified direction close to the line of flight. This direction may deviate slightly from the flight direction so that wind components are resolved around meaningful axes (e.g. along and across the thermal wind in a frontal zone). The dropsonde positions along a particular leg of the aircraft flight are projected on to this plane (Figure 1). The horizontal coordinate of the analysis domain is distance along the projected plane and the vertical coordinate can be either pressure, θ or θ_w.

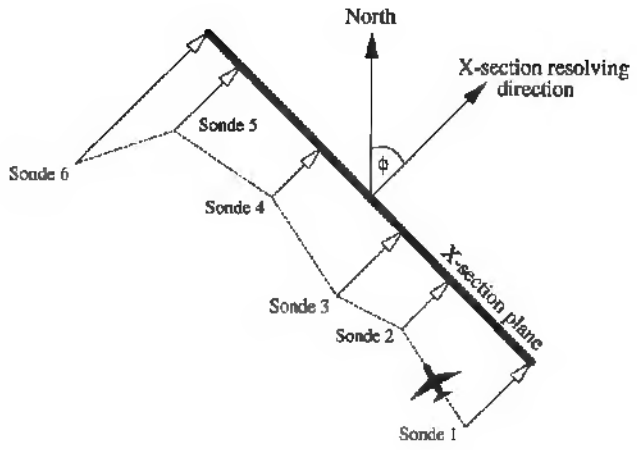

Figure 1 *Plan view schematic of aircraft track (dashed line) showing dropsonde positions and projection onto a vertical plane orientated perpendicular to an angle ϕ.*

3.2 Analysis Method

The analysis equation as defined in P93 (using the same notation) is

$$\mathbf{f}_g^{\,k} = \bar{\mathbf{f}}_g + \Omega_g \, \beta^k \qquad (1)$$

where $\mathbf{f}_g^{\,k}$ is the analysed gridded field at the k^{th} iteration, $\bar{\mathbf{f}}_g$ is the "mean" field on the analysis grid, Ω_g is a normal-error influence weighting function model that transforms the analysis from observation space to the analysis grid, and β^k is a parameter vector that depends only on observed variables, the number of iterations, and the weighting matrix in observation space, Ω_o.

The "mean" field defined on the analysis grid, $\bar{\mathbf{f}}_g$ ($\bar{\mathbf{f}}_o$ is the equivalent defined at observation points) is calculated once at the beginning of the analysis by fitting a 2-dimensional linear trend model to the observations. This field is removed from the observational data, $\mathbf{f}_o$, for the analysis. This removes information on scales larger than the analysis domain so the analysis scheme only attempts to fit scales that are resolved within the domain. The mean field is added back on to the final analysed field at the end of the analysis.

The normal-error influence function model for the analysis grid Ω_g (Ω_o in observation space) is defined as

$$\Omega(x_{ij}) = \exp\left(-{}^1\!/_2 \, (x_{ij} / L)^2\right) \qquad (2)$$

where x_{ij} is the distance between two points i and j in the analysis domain and L is a specified filter scale. Note that Ω_g and Ω_o only need to be defined once at the start of the analysis. The filter function is isotropic but for a 2-dimensional vertical cross-section a different filter scale may be required in each direction. As described in P93

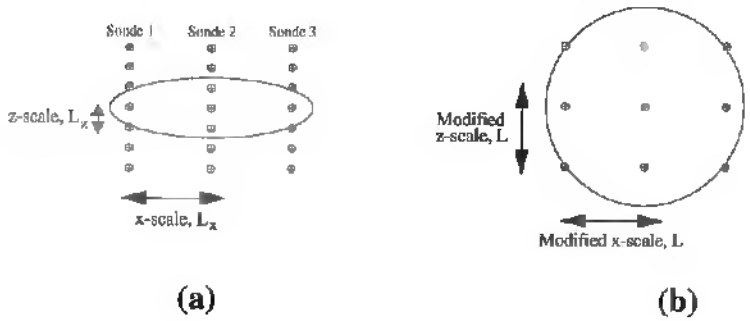

Figure 2 *Schematic of dropsonde data locations (3 dropsondes) in the vertical analysis plane (a) in distance coordinates with an ellipse representing the desired filter scales in each direction (L_x and L_z) and (b) in scaled coordinates so the filter scale is isotropic and can be specified by a single scale, L.*

(Appendix B) this can be achieved by scaling the observation coordinates relative to length scales defined separately for each direction (L_x for the horizontal coordinate and L_z for the vertical coordinate). In the new scaled coordinate system, the filter scale L is defined as unity, so L_x and L_z actually correspond to the filter scales in equation (2) for each direction. See Figure 2 for an illustration. The specification of the filter scales is discussed in more detail in Section 4.

The parameter vector $\boldsymbol{\beta}^k$ contains the iterative part of the analysis method which is performed completely in observation space (i.e. there is no reference to an analysis grid). The iterative equations are

$$\boldsymbol{\beta}^k = \boldsymbol{\beta}^{k-1} + \alpha \mathbf{C}_o^{-1} \mathbf{r}^{k-1} \qquad (3)$$

$$\mathbf{r}^k = (\mathbf{f}_o - \bar{\mathbf{f}}_o) - \boldsymbol{\Omega}_o \boldsymbol{\beta}^k \qquad (4)$$

where $(\mathbf{f}_o - \bar{\mathbf{f}}_o)$ is the vector of detrended observations, α (≥ 1) is an optional over-relaxation parameter and $\mathbf{C}_o$ is a diagonal matrix of normalisation constants.

$$C_{ii} = \sum_{j=1}^{n} \Omega(x_{ij})$$

where n is the number of observations. At each iteration of equations (3) and (4), the analysis field draws closer to the observations at observation points. Once the specified number of iterations has been reached, the analysis values are interpolated onto the analysis grid using the filter, Ω_g, and the mean field is added to produce the final analysis field as described by equation (1).

An objective analysis is performed separately for the four variables measured by the dropsonde: temperature, relative humidity and two perpendicular wind components. For the analysis on θ and θ_w surfaces, the pressure data is also objectively analysed and an extra step interpolates the four main analysed fields from θ or θ_w levels on to pressure levels using the analysed pressure field. Relative humidity (RH) is the only variable not analysed directly; it is transformed to $\sqrt{1-(RH/100)}$ for the analysis. There are two reasons for this. Firstly, it prevents relative humidity becoming negative in the final analysis (because the analysis values are squared to retrieve RH). Secondly, the observations will usually be in moist parts of the atmosphere (high RH) and the transformation biases the sampling to these higher values. The filter scales are also reduced to $^2/_3$ of their value for the RH analysis to avoid excessive smoothing of the large gradients that can occur in this field. An example of the analysis fields for FASTEX IOP16 is shown in Figure 3.

The final step is the calculation of various diagnostics from the four gridded fields on pressure levels (i.e. temperature, relative humidity, wind components). A list of diagnostics is included in Appendix 1.

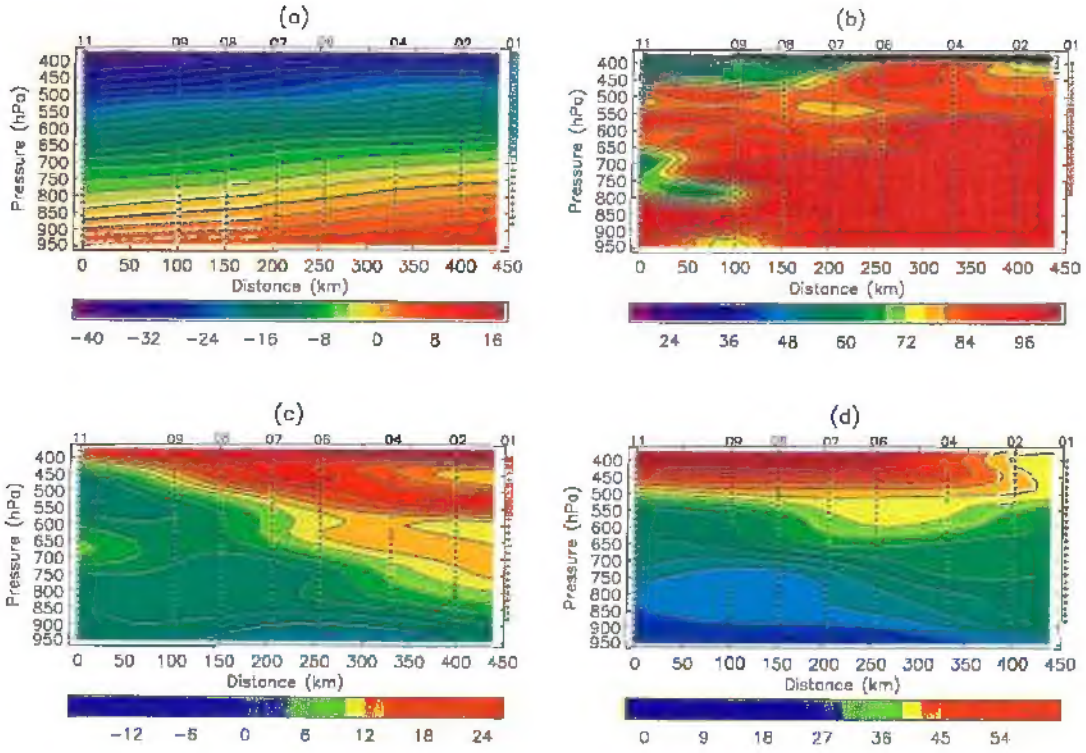

Figure 3 *Pressure surface analysis cross-sections for the first flight leg in FASTEX IOP 16 showing (a) temperature, (b) relative humidity, (c) wind component parallel to the cross-section and (d) wind component perpendicular to the cross-section. Each cross section is overlayed with 20hPa layer average sonde data values which provides a visual estimate of the analysis fit to the data and highlights data sparse regions. A black cross represents each sonde data point, and the surrounding coloured square represents the value at this point using the same colour range as the cross section.*

3.3 Analysis Error

A form of "analysis error" is useful to provide information on the quality of the analysis and where to treat the analysis with caution. Because there is no background field and associated background error, an "analysis error" can only be sensibly defined at observation points. So the most useful information is knowing where the observations are and how well the analysis fits these observations.

One indicator of the analysis fit to the data at the k^{th} iteration is that of the residual increments on observing sites, $\mathbf{r}^k$, defined in Equation (4), and a useful diagnostic is the mean-square residual of $\mathbf{r}^k$. However, this should be treated with caution if the observations have a significant error of representivity for the scales resolved by the analysis. Analysis parameters can be chosen so that the analysis fits the small scales in the observations very closely but a noisy field may result and a smoother analysis with a higher residual error may be considered to be a better analysis. However, the residual, $\mathbf{r}^k$, is more meaningful if the observations have been filtered in the vertical

before the analysis so that only scales resolvable by the analysis are retained (i.e. the error of representivity is small).

A more visual technique is to compare a vertical profile from the analysis with the full resolution dropsonde data or alternatively overlay the sonde data values on the analysis field image. The latter shows the observation locations, highlights data sparse regions where the analysis cannot be trusted, and provides a visual estimate of the spatial variation of the analysis fit to the data (e.g. Fig. 3).

4. Sensitivity of the Analysis to Parameter and Coordinate Changes

There are a number of parameters that need to be defined for the objective analysis, including the filter scales, the smoothing parameter, the number of iterations and the analysis grid resolution. The choice of vertical coordinate (pressure, dry, or moist isentropic surfaces) also has a significant impact on the characteristics of the analyses. The effects of changes to these analysis parameters and coordinates are described in this section.

4.1 Observation Density and Filter Scales

In FASTEX, the dropsonde data distribution along a flight leg is highly inhomogeneous in space with very high resolution in the vertical and relatively low resolution in the horizontal. A typical horizontal separation between dropsondes is 50km, and a typical vertical resolution in each dropsonde profile is 20m. The objective analysis can only represent features that are resolved in both the horizontal and vertical directions. If there are small scale features in the high vertical resolution data that have a horizontal scale significantly less than the distance between dropsondes, then a noisy analysis may result due to the large error of representivity. It is not absolutely necessary to filter the dropsonde data in the vertical to remove these small scales as the analysis can perform this filtering if the appropriate filter scales are specified. However, the objective analysis algorithm is more efficient with less data and is less likely to be influenced by small scale anomalies.

The horizontal filter scale, L_x, is generally limited by the average spacing of dropsondes across the section and must be set to a value comparable to or larger than this separation to obtain a smooth analysis field. In practice, the spacing between dropsondes is often greater than 50km due to sonde failures and a horizontal filter scale of around 100km is used. A choice of vertical coordinate scale, L_z, of 50hPa for pressure surfaces, and 2°C for θ-surfaces gives a reasonably smooth analysis for a typical FASTEX frontal zone.

The analyses generally fit the observations well on the resolvable scales, but the fit tends to be worst where observations on a particular analysis level alternate between high and low values on consecutive dropsondes. The relative humidity field is particularly susceptible to this as there can be steep gradients along a pressure or

isentropic surface. An example can be seen between sonde 8 and sondes 7 and 9 at 500hPa in Figure 3b.

The impact of decreasing the horizontal separation of dropsondes has been assessed by taking pseudo-soundings from a Unified Model mesoscale integration of FASTEX IOP 16 with horizontal resolution of about 11km and a vertical resolution of about 25hPa. The soundings were sampled at different horizontal intervals and objectively analysed cross section were formed (one example is shown in Figure 4). The results show that a dropsonde spacing of 60km is high enough resolution for the objective analysis to resolve the features in the model cross section, and little is gained by extracting more sondes with decreased separation. This confirms that the mesoscale model is not resolving scales much smaller than 60km, but this result cannot be extrapolated to the real atmosphere in which there are atmospheric features on all scales. However, it does suggest that the spacing of sondes in FASTEX is adequate to resolve similar scales to those expected from the 11km resolution mesoscale model.

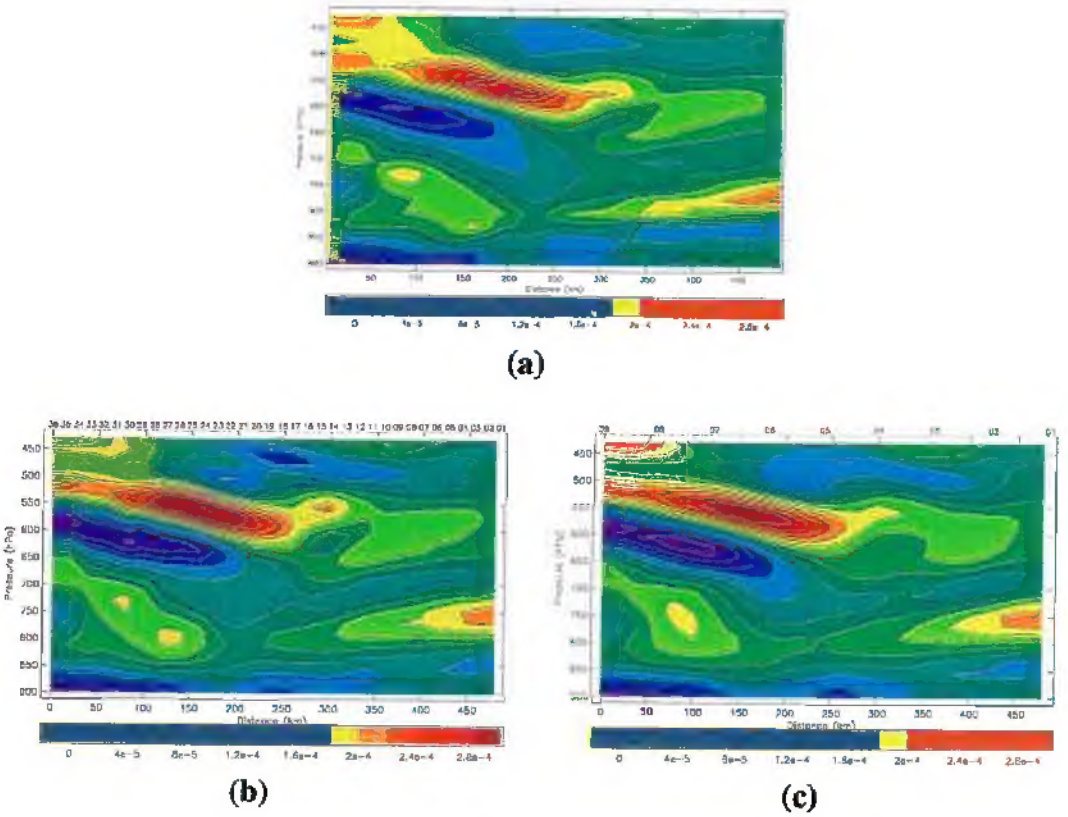

Figure 4 *(a) Cross section of dry static stability from a mesoscale model with 11km resolution in the horizontal and approximately 25hPa resolution in the vertical (45 levels). (b) and (c) show derived static stability from a pressure coordinate objective analysis of dropsondes extracted from this model cross section.(b) Objective analysis with 36 sondes (15km separation) and a filter scale of 15km. (c) Objective analysis with 9 sondes (60km separation) and a filter scale of 60km.*

4.2 Vertical Coordinate

The FASTEX dropsonde measurements are mainly in frontal zones and atmospheric features in these regions tend to be sloping along dry isentropic (θ) or moist isentropic (θ_w) surfaces. One limitation of the analysis method is that the filter scales can only be defined along the horizontal coordinate and vertical coordinate directions, so a pressure surface analysis with pressure as the vertical coordinate is often unable to coherently represent features on sloping isentropes. One solution is to define the analysis vertical coordinate as θ or θ_w. Figure 5 illustrates the effect of varying the orientation of the anisotropic filter scale from pressure surfaces to isentropic surfaces and highlights the potential improvement, if the atmospheric features being analysed are sloping along isentropes. An example can be seen in the vertical gradient of potential temperature ($d\theta/dz$) for the first flight leg of IOP 16. Figure 6 shows this field for analyses on pressure, θ, and θ_w-surfaces. $d\theta/dz$ is shown as it is a derivative field and is particularly sensitive to the analysis characteristics. There is a shallow band of high $d\theta/dz$ in all the sondes from 1 to 7 sloping from 450hPa in sonde 7 to 550hPa in sonde 1. Figure 6(a) shows the gradient field derived from an analysis on pressure surfaces. The band of high $d\theta/dz$ is broken into two bands along pressure surfaces in the upper right hand corner of the domain. The θ-surface analysis (Fig. 6b) produces a coherent sloping structure with a closer fit to the data. The θ_w-surface analysis (Fig. 6c) is the worst fit, partly because θ_w becomes multivalued over a significant part of the domain but also because there has been less optimisation of the analysis parameters. In regions where the atmospheric flow is expected to be along steeply sloping θ_w surfaces the θ_w-surface analysis is able to represent features along these slopes but the problem of defining a monotonic grid coordinate for the whole domain remains.

The $d\theta/dz$ field is a particularly stringent test of the analysis and although there are differences between other fields analysed on pressure and θ–surfaces, they are often less obvious. Figure 7 shows the four directly analysed fields (temperature, relative humidity and wind components) for the first flight leg in IOP 16 analysed on θ-surfaces for comparison with Figure 3.

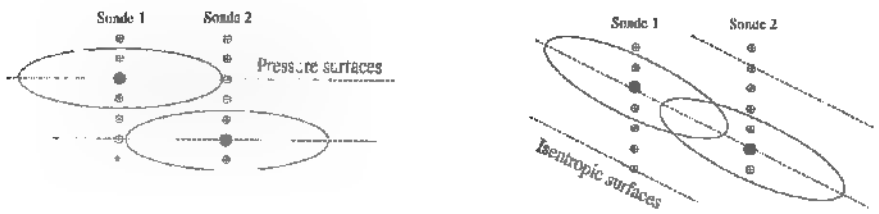

(a) **(b)**

Figure 5 *Schematic of dropsonde data locations in the vertical analysis plane in distance coordinates with a sloping feature highlighted in the sondes (solid circles). An ellipse represents the anisotropic filter scales for an analysis on (a) pressure surfaces, and (b) isentropic surfaces.*

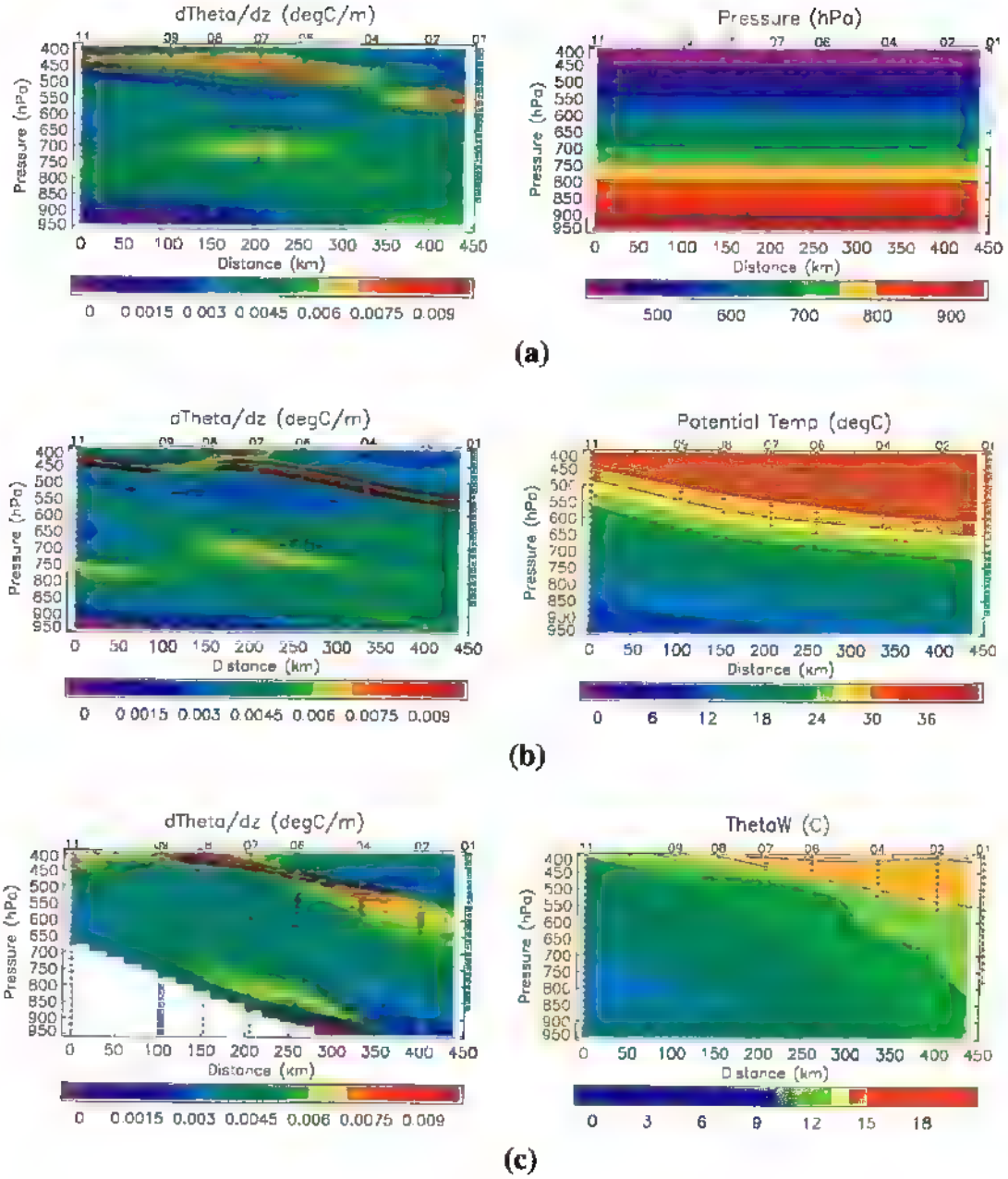

Figure 6 *Vertical gradient of potential temperature for the first flight leg in FASTEX IOP 16 (left hand side) and vertical coordinate (right hand side) for analyses on (a) pressure levels, (b) θ levels and (c) θ_w levels. Where levels cannot be defined in the θ_w-level analysis (c) the field is blanked out. Each cross section is overlayed with 20hPa layer average sonde data values which provides a visual estimate of the analysis fit to the data and highlights data sparse regions. A black cross represents each sonde data point, and the surrounding coloured square represents the value at this point using the same colour range as the cross section.*

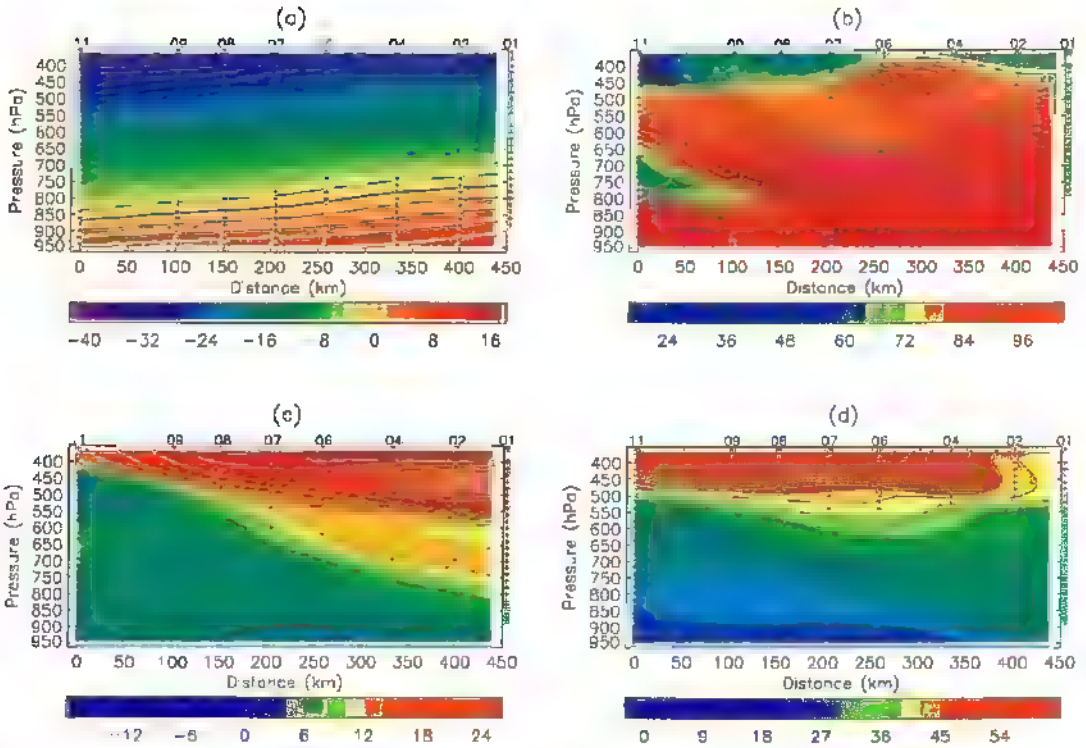

Figure 7 *As Figure 3 but with objectively analysed cross-sections on isentropic surfaces showing (a) temperature, (b) relative humidity, (c) wind component parallel to the cross-section and (d) wind component perpendicular to the cross-section.*

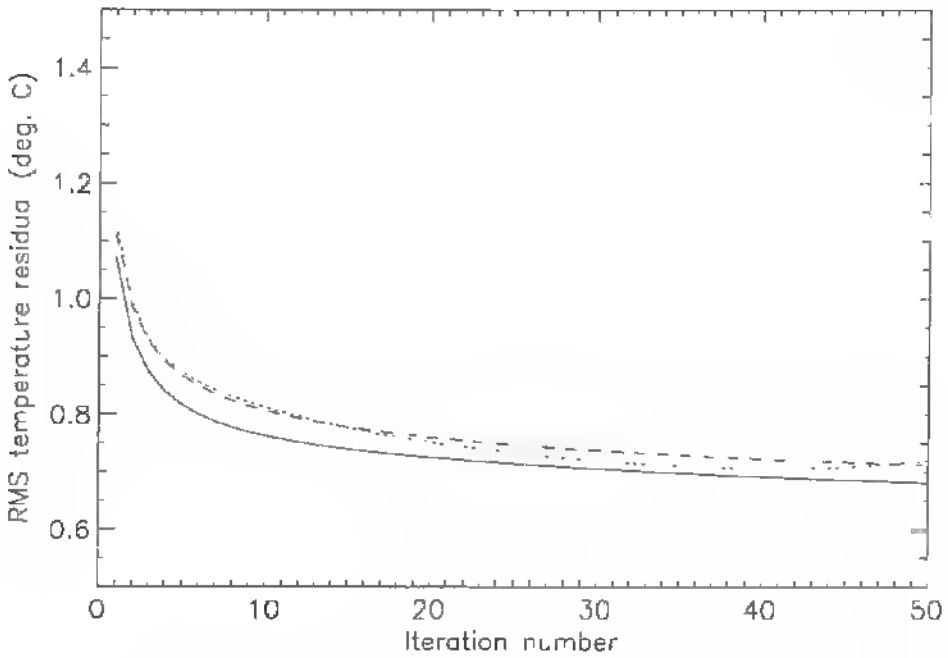

Figure 8 *Evolution of the root-mean-square temperature residual (i.e. the difference between the analysis and observations) for the first flight leg in IOP 16 as the analysis iteration number increases. Each line is for a different value of the over-relaxation parameter α; α=1.9 (solid), α=1.0 (dashed), α=2.1(dotted).*

4.3 Other analysis parameters

The rate of convergence of the analysis to the observations is high for the first few iterations but decreases rapidly after this. Figure 8 shows the evolution of the root-mean-square of the residual temperature, $\mathbf{r}^k$, at observation points as the iterations progress. The analysis is found to be close to convergence after about 50 iterations without overfitting. The over-relaxation parameter, α, controls the rate of convergence and should have a value between 1.0 and 2.0. The rate of convergence can be increased in the early iterations by increasing α, but a value greater than 2.0 begins to degrade the analysis in later iterations. An optimal value of 1.9 speeds convergence whilst having a minimal detrimental impact on analysis accuracy. The different rates of convergence are highlighted in Figure 8 for values of α equal to 1.0, 1.9, and 2.1.

The resolution of the analysis grid should be comparable or higher than the scales expected to be resolved by the analysis, defined by the effective filter scale in each direction. A typical grid resolution used for the FASTEX dropsonde analyses is 20km in the horizontal and 200m in the vertical.

The recommended parameter values for an objective analysis of FASTEX dropsonde data are summarised in Table 1.

Description	Recommended Value
Number of iterations, k	50
Over-relaxation parameter, α	1.9
Analysis grid resolution	20km x 200m
Horizontal coordinate filter scale, L_x	100km
Vertical coordinate filter scale, L_z	p=50hPa or θ=2°C

Table 1 *List of recommended values for analysis parameters for typical FASTEX dropsonde cross sections.*

5. Concluding Discussion

A successive correction technique has been used to objectively analyse dropsondes along aircraft flight legs in FASTEX and produce vertical cross-sections of various atmospheric fields. The characteristics and sensitivities of the objective analysis method have been investigated in the context of the FASTEX dropsonde data. The analysis method fits the data well and adequately resolves major features with horizontal length scales around 50km and vertical scales around 500m. The horizontal distance between adjacent dropsondes is the limiting factor for resolving smaller scale features in the analyses.

It is apparent that the coordinate system used in the analysis does have a significant impact on the resulting analyses for the typical data distributions in FASTEX. Out of the three analysis coordinates, defining the vertical coordinate as potential temperature appears to be the best compromise for representing atmospheric features in frontal zones, although the other analysis coordinates may also provide useful information. There are other possible coordinates, such as a hybrid θ / θ_w vertical coordinate or a momentum horizontal coordinate, which will produce slightly different analyses yet again, but with the limited horizontal resolution of observations it is difficult to say which would result in the "best" analysis and this may vary with the particular case under study.

A final remark is a word of caution. There are some regions with very little data due to multiple dropsonde failures and the analyses can be misleading in such regions. The other issue to be aware of is the time difference across the section. Although the sondes along a flight leg are generally all within an hour or so of each other there will be some evolution of the meteorological fields during this time.

Despite these difficulties, the objective analysis system provides an automated "best" estimate of a spatially coherent field given the available observations and is a valuable aid to visualising the atmosphere.

Appendix 1. Diagnostics available from the dropsonde objective analysis

Temperature and relative humidity based diagnostics

* Temperature
  Dry bulb potential temperature (θ)
  Wet bulb potential temperature (θ_w)
  Equivalent potential temperature (θ_e)
  Saturated equivalent potential temperature
  Along section derivative of θ ($d\theta/dx$)
  Along-section derivative of θ ($d\theta_e/dx$)
  Vertical derivative of θ ($d\theta/dz$)
  Vertical derivative of θ_e ($d\theta_e/dz$)
  Dry static stability (Brunt-Vaisala frequency)
  Moist static stability (Brunt-Vaisala frequency)
  Dry Richardson Number.
  Moist Richardson. Number
* Relative humidity with respect to water
  Relative humidity with respect to ice
  Ice supersaturation
  Specific Humidity
  Dew Point
  Frost Point
  Humidity mixing ratio
  Density

Wind based diagnostics

* Along-section wind (u component)
* Across-section wind (v component)
  Along-section wind (u component) relative to system velocity
  Along-section wind (v component) relative to system velocity
  Vertical derivative of along-section wind component (du/dz)
  Vertical derivative of along-section wind component (dv/dz)
  Wind direction
  Wind strength
  Momentum

2D diagnostics of 3D quantities - these diagnostics must be treated with great caution as they are based on a 2-dimensional velocity field

  Divergence
  Dry potential vorticity
  Moist potential vorticity
  Absolute vorticity

* primary variable objectively analysed directly, all others are diagnosed from the primary variables

REFERENCES

Bratseth, A. M., 1986: Statistical interpolation by means of successive corrections. *Tellus*, **38** (A), 439-447.

Cressman, G., 1959: An operational objective analysis system. *Mon. Wea. Rev.*, **88**, 327-342.

Daley, R., 1991: *Atmospheric Data Analysis*. Cambridge University Press.

Desroziers,G. and J.-P. Lafore, 1993: A coordinate transformation for objective frontal analysis. *Mon. Wea. Rev.*, **121**, 1531-1553.

Harmer, J., Kilsby, C. G., Rudman, S. R., Seymour, J. H., 1990: Temperature measurements on the C130 - working group report. *MRF Internal Note 55*, U.K. Met. Office.

Joly, A., D. Jorgensen, M. A. Shapiro, A. Thorpe, P. Bessemoulin, K. A. Browning, J.-P. Cammas, J.-P. Chalon, S. A. Clough, K. A. Emanuel, L. Eymard, R. Gall, P. H. Hildebrand, R. H. Langland, Y. Lemaitre, P. Lynch, J. Moore, P. O. G. Persson, C. Snyder, R. M. Wakimoto, 1997: The Fronts and Atlantic Storm-Track Experiment (FASTEX): Scientific objectives and experimental design. *Bull. Amer. Meteor. Soc.*, **78**, 1917-1940.

Offiler, D., P. R. A. Brown, A. L. M. Grant, W. D. N. Jackson, D. W. Johnson, 1994: Report of the aircraft winds working group. *MRF Technical Note 17*, U.K. Met. Office.

Pedder, M. A., 1993: Interpolation and filtering of spatial observations using successive corrections and Gaussian filters. *Mon. Wea. Rev.*, **121**, 2889-2902.

Rogers, D. P., 1995: The stable internal boundary layer over a coastal sea. Part I: Airborne measurements of the mean and turbulence structure. *J. Atmos. Sci.*, **52**, 667-683.

Shapiro, M. A., and J. T. Hastings, 1973: Objective cross-section analyses by Hermite polynomials interploated on isentropic surfaces. *J. App. Meteor.*, **12**, 753-762.

CURRENT JCMM INTERNAL REPORTS

This series of JCMM Internal Reports, initiated in 1993, contains unpublished reports and also versions of articles submitted for publication. The complete set of Internal Reports is available from the National Meteorological Library on loan, if required.

1. **Research strategy and programme**
   K A Browning et al
   January 1993

2. **The GEWEX Cloud System Study (GCSS)**
   GEWEX Cloud System Science Team
   January 1993

3. **Evolution of a mesoscale upper tropospheric vorticity maximum and comma cloud from a cloud-free two dimensional potential vorticity anomaly**
   K A Browning
   January 1993

4. **The global energy and water cycle**
   K A Browning
   July 1993

5. **Structure of a midlatitude cyclone before occlusion**
   K A Browning and N Roberts
   July 1993

6. **Developments in systems and tools for weather forecasting**
   K A Browning and G Szejwach
   July 1993

7. **Diagnostic study of a narrow cold frontal rainband and severe winds associated with a stratospheric intrusion**
   K A Browning and R Reynolds
   August 1993

8. **Survey of perceived priority issues in the parametrizations of cloud-related processes in GCMs**
   K A Browning
   September 1993

9. **The effect of rain on longwave radiation**
   I Dharssi
   September 1993

10. **Cloud microphysical processes - a description of the parametrization used in the large eddy model**
    H Swann
    October 1993

11. **An appreciation of the meteorological research of Ernst Kleinschmidt**
    A J Thorpe
    May 1992

12. **Potential vorticity of flow along the Alps**
    A J Thorpe, H Volkert and Dietrich Heimann
    August 1992

13. **The representation of fronts**
    A J Thorpe
    January 1993

14. **A parametrization scheme for symmetric instability: test for an idealised flow**
C S Chan and A J Thorpe
February 1993

15. **The Fronts 92 Experiment: a Quicklook Atlas**
Edited by T D Hewson
November 1993

16. **Frontal wave stability during moist deformation frontogenesis**
Part 1: Linear wave dynamics
C H Bishop and A J Thorpe
May 1993

17. **Frontal wave stability during moist deformation frontogenesis**
Part 2. The suppression of non-linear wave development
C H Bishop and A J Thorpe
May 1993

18. **Gravity waves in sheared ducts**
S Monserrat and A J Thorpe
October 1993

19. **Potential vorticity and the electrostatics analogy: quasi-geostrophic theory**
C Bishop and A J Thorpe
November 1993

20. **Recent advances in the measurement of precipitation by radar**
A J Illingworth
April 1993

21. **Micro-physique et givrage: cloud microphysics and aircraft icing**
A J Illingworth
May 1993

22. **Differential phase measurements of precipitation**
M Blackman and A J Illingworth
May 1993

23. **Estimation of effective radius of cloud particles from the radar reflectivity**
N I Fox and A J Illingworth
May 1993

24. **A simple method of Dopplerising a pulsed magnetron radar**
A Hua, A J Illingworth and J Eastment
November 1993

25. **Radiation and polar lows**
George C Craig
February 1994

26. **Collected preprints submitted to the International Symposium on the Life Cycles of Extratropical Cyclones; Bergen, Norway, 27 June - 1 July 1994**
April 1994

27. **Convective frontogenesis**
Douglas J Parker and Alan J Thorpe
April 1994

28. **Improved measurement of the ice water content in cirrus using a total water evaporator**
Philip R A Brown and Peter N Francis
April 1994

29. **Mesoscale effects of a dry intrusion within a vigorous cyclone**
K A Browning and B W Golding
April 1994

30. **GEWEX Cloud System Study, Science Plan**
May 1994

31. **Parametrization of momentum transport by convectively generated gravity waves**
R Kershaw
May 1994

32. **Mesoscale Modelling Newsletter No 5**
May 1994

33. **Observations of the mesoscale sub-structure in the cold air of a developing frontal cyclone**
K A Browning, S A Clough, C S A Davitt, N M Roberts and T D Hewson
May 1994

34. **Longwave radiative forcing of a simulated tropical squall line**
Imtiaz Dharssi
July 1994

35. **On the nature of the convective circulation at a kata-cold front**
K A Browning
September 1994

36. **Collective preprints of papers submitted to the COST-75 International Seminar on Advanced Weather Radar Systems, Brussels, 20-23 September 1994**
November 1994

37. **Use of satellite imagery to diagnose events leading to frontal thunderstorms: Parts I and II of a case study**
K A Browning and N M Roberts
November 1994

38. **The role of spaceborne millimetre-wave radar in the global monitoring of ice cloud**
P R A Brown, A J Illingworth, A J Heymsfield, G M McFarquhar, K A Browning and M Gosset
December 1994

39. **Potential vorticity inversion**
Michal Ziemianski
October 1994

40. **Theory of mature tropical cyclones; a comparison between Kleinschmidt (1951) and Emanuel (1986)**
Suzanne L Gray
December 1994

41. **Dispersion and removal of pollutants during the passage of an atmospheric frontal system**
N R Gimson
December 1994

42. **The role of snow sublimation in frontogenesis**
D J Parker and A J Thorpe
December 1994

43. **Potential vorticity and the electrostatics Analogy: Ertel-Rossby formulation**
A J Thorpe and C H Bishop
December 1994

44. **Mesoscale aspect of extratropical cyclones: an observational perspective**
K A Browning
January 1995

45. **A polar low outbreak: evolution and mesoscale structures**
T D Hewson, G C Craig and C Claud
February 1995

46. **Generation of near-surface gusts of deep convection**
K Nakamura and R Kershaw
April 1995

47. **Attribution concepts applied to the Omega Equation**
S A Clough, C S A Davitt and A J Thorpe
June 1995

48. **Parametrization of mixed-phase cloud and precipitation**
Susan P Ballard and M Gerard Hutchinson
June 1995

49. **Short-range forecasting of stratocumulus: initialization prediction**
Susan P Ballard, Simon D Jackson and B Macpherson
June 1995

50. **Contributions of the JCMM/Dept of Meteorology Radar Group to the 27th AMS Radar Meteorology Conference, Vail October 1995**
June 1995

51. **Cold pools in shear**
Douglas J Parker
September 1995

52. **High-resolution analysis of frontal fracture**
K A Browning, S P Ballard and C S A Davitt
September 1995

53. **The albedo of broken cloud fields: calculations using a modified two stream radiation code**
Imtiaz Dharssi and Roy Kershaw
October 1995

54. **Parametrization of momentum transport by convection. I: theory and cloud modelling results**
R Kershaw and D Gregory
November 1995

55. **Variation of frontal structure along a cold front**
K A Browning and N M Roberts
November 1995

56. **Secondary frontal waves**
Douglas Parker
December 1995

57. **Objective fronts**
T D Hewson
March 1996

58. **Mesoscale analysis of the activation of a cold front during cyclogenesis**
K A Browning, N M Roberts and A J Illingworth
June 1996

59. **Investigation of different representations of rain in a 1-d evaporation model**
H Swann
May 1996

60. **Parametrization of diabatic processes in the inversion of the omega-equation**
M Athanassiadou and A J Thorpe
June 1996

61. **The role of the environmental flow in the development of secondary frontal cyclones**
I A Renfrew, A J Thorpe and A Joly
June 1996

62. **Consequences of the geostrophic momentum approximation on barotropic instability**
S Malardel, A J Thorpe and A Joly
June 1996

63. **Contributions to the AMS/RMS Conference on Mesoscale Processes**
Reading, 9-13 September 1996

64. **Vorticity and potential vorticity in stratified flows interacting with an isolated obstacle**
Jorge A Gutiérrez and A J Thorpe
September 1996

65. **Triple point development: two case studies**
Douglas Parker
September 1996

66. **Radar observations of wind-shear splitting within evolving atmospheric Kelvin-Helmholtz billows**
D Chapman and K A Browning
April 1997

67. **Cold frontal structure derived from radar wind profilers**
K A Browning, D Jerrett, J Nash, T Oakley and N M Roberts
May 1997

68. **The dry intrusion and its effect on the frontal, cloud and precipitation structure of extratropical cyclones**
K A Browning - Text of invited special lecture at the Spring Conference of the Meteorological Society of Japan, University of Tsukuba, 22 May 1997

69. **Met. Office Unified Model data, diagnostics, graphics programs, and other observational data available from the JCMM through the aegis of the Universities Weather Research Network (UWERN).** (Plus supplement)
Peter Panagi and Ed Dicks
June 1997

70. **Contributions of the JCMM/Dept of Meteorology Radar Group to the 28th AMS Radar Meteorology Conference.** Austin, Texas
September 1997

71. **Sensitivity of short-range weather forecasts to local potential vorticity modifications**
Meral Demirtas and Alan Thorpe
July 1997

72. **Objective identification of frontal wave cyclones**
T D Hewson
August 1997

73. **Attribution and its application to mesoscale structure associated with tropopause folds**
A J Thorpe
September 1997

74. **The role of the environmental flow in the development of secondary frontal cyclones**
Ian A Renfrew, Alan J Thorpe and Craig H Bishop
September 1997

75. **Potential vorticity: a short history of its definitions and uses**
Alan J Thorpe and Hans Volkert
September 1997

76. **Superposing semi-geostrophic potential vorticity anomalies**
H R Birkett and A J Thorpe
September 1997

77. **Short period forecasting of catchment-scale precipitation.**
Part 1: the role of Numerical Weather Prediction
M A Pedder, M Haile and A J Thorpe
September 1997

78. **Verification of the tracking technique used in an experimental cloud motion wind inferring system**
Z Wang, K A Browning and G A Kelly
October 1997

79. **A preliminary study of Fourier series analysis for cloud tracking with GOES high temporal resolution images**
Z Wang
October 1997

80. **Analysis of an ex-tropical cyclone after reintensifying as a warm-core extratropical cyclone**
K A Browning, G Vaughan and P Panagi
November 1997

81. **A JCMM overview of FASTEX IOPs**
S A Clough, H W Lean, N M Roberts, H Birkett, J-P Chaboureau, R Dixon, M Griffiths, T D Hewson and A Montani
January 1998

82. **Programs for PV inversion and modification**
Meral Demirtas
December 1997

83. **Release of potential shearing instability in warm frontal zones**
D Chapman and K A Browning
February 1998

84. **The European Cloud-Resolving Modelling Programme (EUCREM)**
Summary Report from the coordinator
P W White
April 1998

85. **A frontal wave database**
T D Hewson
April 1998

86. **Layering observed in dropsoundings from IOP 1 of Fronts 92**
S A Clough
May 1998

87. **Use of wind-shear displays for Doppler radar data**
D Chapman and K A Browning
May 1998

88. **Radar estimates of rainfall rates at the ground in bright band and non-bright band events**
T J Smyth and A J Illingworth
June 1998

89. **Correction for attenuation of radar reflectivity using polarisation data**
T J Smyth and A J Illingworth
June 1998

90. **The effects of convection on chemical reactions and precipitation scavenging**
Neil R Gimson
July 1998

91. **How to use the display program DISP**
Nigel Roberts
August 1998

92. **Conceptual models of cyclogenesis**
Adrian T Semple
August 1998

93. **Observations of oblate hail using dual polarisation radar and implications for hail detection schemes**
T J Smyth, T M Blackman and A J Illingworth
September 1998

94. **The semigeostrophic diagnosis of vertical motion. Part I: Formulation and co-ordinate transformations**
Mike A Pedder and Alan J Thorpe
September 1998

95. **The semigeostrophic diagnosis of vertical motion. Part II: Results for an idealised baroclinic wave life cycle**
Alan J Thorpe and Mike A Pedder
September 1998

96. **Convective destabilisation by a tropopause fold diagnosed using potential vorticity inversion**
Morwenna Griffiths, Alan Thorpe and Keith Browning
October 1998

97. **Forecast skill of the ECMWF model using targeted observations during FASTEX**
A Montani, A J Thorpe, R Buizza and P Unden
October 1998

98. **Observations and model simulations of the FASTEX IOP 16 frontal wave - effects of sublimation**
Sid A Clough, Humphrey W Lean, Nigel M Roberts and Richard M Forbes
December 1998

99. **The application of conceptual models in NWP**
Adrian T Semple
January 1999

100. **Mesoscale analysis of arc rainbands in a dry slot**
K A Browning and N M Roberts
January 1999

101. **Interaction of mesoscale tropopause depressions with a warm-core cyclone: observational and model analyses, and sensitivity to analysis errors**
K A Browning, A J Thorpe, A Montani, D Parsons, M Griffiths, P Panagi and E M Dicks
February 1999

102. **Use of water vapour imagery and PV inversion to adjust initial conditions in NWP**
Sean J Swarbrick
February 1999

103. **Summary notes for a lecture course on Waves in the Atmosphere and Ocean**
A A White
March 1999

104. **Results of a questionnaire on the operational value of conceptual models (CMs) of fronts and cyclones**
N M Roberts & M V Young
July 1999

105. **Contributions to the Poster Session at the 1998 UWERN Annual Science Meeting**
assembled by A A White
August 1999

106. **The objective analysis of dropsonde data from FASTEX**
Richard Forbes, Sid Clough, Mark Dixon, Andy Macallan & Nigel Roberts
January 2000

Met Office Joint Centre for Mesoscale Meteorology Department of Meteorology
University of Reading PO Box 243 Reading RG6 6BB United Kingdom
Tel: +44 (0)118 931 8425 Fax: +44 (0)118 931 8791
www.metoffice.com